Coalescence Dynamics of Deformable Brownian Emulsion Droplets

K. D. Danov,† N. D. Denkov,† D. N. Petsev,† I. B. Ivanov,*,† and R. Borwankar‡

Laboratory of Thermodynamics and Physico-chemical Hydrodynamics, Faculty of Chemistry, Sofia University, 1126 Sofia, Bulgaria, and Kraft General Foods, Inc., 801 Waukegan Road, Glenview, Illinois 60025

Received January 25, 1993. In Final Form: May 5, 1993

The Smoluchowski approach for treatment of diffusion-controlled coagulation is modified to include the case of coalescing emulsion droplets which can deform before flocculation or coalescence. By using appropriate expressions for the droplet interaction and boundary conditions of Smoluchowski type, we calculate the distance at which the droplet deformation takes place, the nonequilibrium (but steady) radial distribution function, and the total force (including the ensemble averaged Brownian force) acting between the droplets. As a result the particle flux toward a given "central" droplet, i.e. the coalescence rate, is determined. The influence of different factors (Hamaker constant, surface potential, interfacial tension, drop size, and others) is investigated numerically.

1. Introduction

The first general treatment of the coagulation kinetics in colloidal systems was performed by Smoluchowski.[1] The theoretical approach, formulated by him, provides a background for studying the so-called diffusion-controlled reactions. A basic feature of all diffusion-controlled processes is the fact that their rates depend on the diffusion approach of the reacting species. Hence, from a mathematical standpoint, diffusion-controlled reactions present a diffusion problem with boundary conditions determined by the specific features of the physicochemical transformation of the contacting molecules, ions, colloidal particles, etc.[2] Smoluchowski theory has been a subject of numerous improvements and generalization:[3-13] both direct interactions between the reacting particles[7,8] and hydrodynamic interactions[9,10] have been incorporated in it. A further step in generalizing the Smoluchowski theory was to take into consideration higher order correlations in the particle positions.[11,12] The deviation of the particle velocity distribution from the Maxwellian type has been also considered by using the Fokker–Planck approach.[13] Recently, Zhang and Davis[14] used the Smoluchowski method to calculate the collision rate for nondeformable droplets, with tangentially mobile surfaces in the absence of surfactants.

All aforementioned theoretical works deal only with nondeformable particles. It is known, however, that the deformability of certain colloids (e.g. microemulsion or emulsion droplets) can significantly affect both the thermodynamic[15] and dynamic properties of these systems. When two large emulsion drops are approaching each other, a thin planar film may form between them.[16] The rate of thinning of this film and its stability against rupture are among the main factors determining the overall stability of the emulsion.[16-18] The role of different factors (like the film radius and thickness, presence of surfactants, etc.) on thin film behavior has been investigated theoretically and experimentally; for a review see, e.g., ref 18. Most of the works on liquid film stability in emulsions deal with relatively large drops (millimeter and submillimeter size), where the effect of the Brownian motion is negligible. Such systems are usually called *macroemulsions*. The case of emulsions consisting of droplets of submicrometer to at most a few micrometers in size has been much less investigated (we call these systems *miniemulsions*). In particular, it is not known in advance whether or not the small droplets (possessing considerably greater capillary pressure) will deform upon mutual approach. Recently, an experimental study of miniemulsion stability was performed by Hofman and Stein.[19] The results were interpreted as an indication for the importance of the droplets deformability for the emulsion stability. Although the authors carried out some calculations of the interaction energy between two deformed droplets, they did not relate this energy to the kinetic constants characterizing coalescence.

We believe that a more rigorous theoretical approach based on the classical model of Smoluchowski[1] should be developed for quantitative treatment of the coalescence rate in miniemulsions. The present study is a step in this direction. The drop–drop interaction due to the joint action of the direct (interparticle) and hydrodynamic forces on one hand, and the Brownian force on the other is studied in more detail. The problem concerning the direct interactions of deformable particles is not a trivial one and represents a separate interest. It was described by us

† Sofia University.
‡ Kraft General Foods, Inc.

(1) Smoluchowski, M. *Phys. Z.* **1916**, *17*, 557; *Phys. Z.* **1916**, *17*, 785; *Z. Phys. Chem.* **1917**, *92*, 129.
(2) Collins, F. C.; Kimball, G. E. *J. Colloid Sci.* **1949**, *4*, 452.
(3) Ovchinnikov, A. A.; Timasheff, S. F.; Belyy, A. A. *Kinetics of Diffusion Controlled Chemical Processes*; Nova Scientific: Commack, NY, 1989.
(4) Calef, D. F.; Deutch, J. M. *Annu. Rev. Phys. Chem.* **1983**, *34*, 493.
(5) Weiss, G. H. *J. Stat. Phys.* **1986**, *42*, 3.
(6) Keizer, J. *Chem. Rev.* **1987**, *87*, 167.
(7) Debye, P. M. *Trans. Electrochem. Soc.* **1942**, *82*, 265.
(8) Fuchs, N. A. *Z. Phys.* **1934**, *89*, 736.
(9) Deutch, J. M.; Felderhof, B. U. *J. Chem. Phys.* **1973**, *59*, 1669.
(10) Derjaguin, B. V. *Theory of Stability of Colloids and Thin Films*; Plenum Press: New York, 1989.
(11) Waite, T. R. *Phys. Rev.* **1957**, *107*, 461; *J. Chem. Phys.* **1958**, *28*, 103.
(12) Wilemski, G.; Fixman, M. *J. Chem. Phys.* **1973**, *58*, 4009.
(13) Titulaer, V. M. *Physica A* **1980**, *100*, 251.
(14) Zhang, X.; Davis, R. H. *J. Fluid Mech.* **1991**, *230*, 479.
(15) Denkov, N. D.; Kralchevsky, P. A.; Ivanov, I. B.; Vassilieff, C. S. *J. Colloid Interface Sci.* **1991**, *143*, 157.
(16) Ivanov, I. B. *Pure Appl. Chem.* **1980**, *52*, 1241.
(17) Ivanov, I. B.; Dimitrov, D. S.; Somasundaran, P.; Jain, R. K. *Chem. Eng. Sci.* **1985**, *44*, 137.
(18) Ivanov, I. B.; Dimitrov, D. S. In *Thin Liquid Films*; Ivanov, I. B., Ed.; Marcel Dekker: New York, 1988; p 379.
(19) Hofman, J. A. M. H.; Stein, H. N. *J. Colloid Interface Sci.* **1991**, *147*, 508.

0743-7463/93/2409-1731$04.00/0

in more detail in a separate paper,[20] where an explicit expression for the van der Waals energy of interaction between two deformed drops (with the shape of spherical segments) was derived. The electrostatic repulsion was also considered and approximate formulas were obtained. In the present paper we show that due to the interparticle interactions and Brownian force the miniemulsion droplets may deform when they come close to each other. A transcendental algebraic equation for the distance at which the deformation takes place (if it does) is derived. The processes of film formation, thinning, and rupture between two colliding droplets are included as separate stages in the Smoluchowski scheme and the flux of coalescing particles is determined.

The theory predicts that with significant long range repulsion (e.g. electrostatic) between the droplets, deformation will not occur. We should emphasize, that there is a qualitative difference between the coagulation behavior of deformable and nondeformable particles. It is due to the presence of deformation energy, as well as to the fact that the direct and hydrodynamic interactions depend significantly on the droplet shape.[20] Such important processes as the surfactant transport and the rupture of the liquid layer between the droplets are also strongly dependent on the geometry of the system and a theory describing them for nondeformed droplets is not yet available. That is why in this study we investigate mainly the case of deformable droplets. The interaction and coalescence rate in miniemulsions of nondeformable droplets in the presence of surfactants will be considered in a subsequent paper.

The article is organized as follows: in section 2 the method of Smoluchowski is applied to deformable emulsion droplets. General equations are derived for the interparticle distance at which the deformation takes place, for the pair probability function, and for the force acting between the droplets; in section 3 the potential energy of interaction and hydrodynamic resistance to the approach of two deformable droplets are considered; the numerical results are presented and discussed in section 4; the conclusions are summarized in section 5.

2. Mutual Diffusion of Deformable Interacting Emulsion Droplets

2.1. A General Diffusion Scheme for Deformable Miniemulsion Droplets. When two *macroemulsion* drops approach each other, deformation of the latter takes place at a distance h_i between their forepoints.[17,18] This quantity and the further dynamics of the film thinning are strongly dependent on the viscous resistance in the gap between the drops. Often, in the beginning of the deformation the drop caps acquire a bell-shaped form called a dimple.[17,18] After that the surfaces in the zone between the drops flatten and a planar film forms. This film thins with time and at a certain critical thickness ruptures.[16-18] If the film can be thermodynamically stable, the thinning stops at the equilibrium thickness h_e where the disjoining pressure in the film equilibrates the capillary pressure in the drops. In this study we consider only the case of thermodynamically unstable films which always rupture: then the film lifetime depends mainly on the rate of thinning and the critical thickness h_{cr}.

In the case of miniemulsions, collisions occur due to Brownian motion. Following Smoluchowski[1,3,7] we consider the diffusion of *deformable miniemulsion* droplets toward a given "central" droplet in the presence of direct

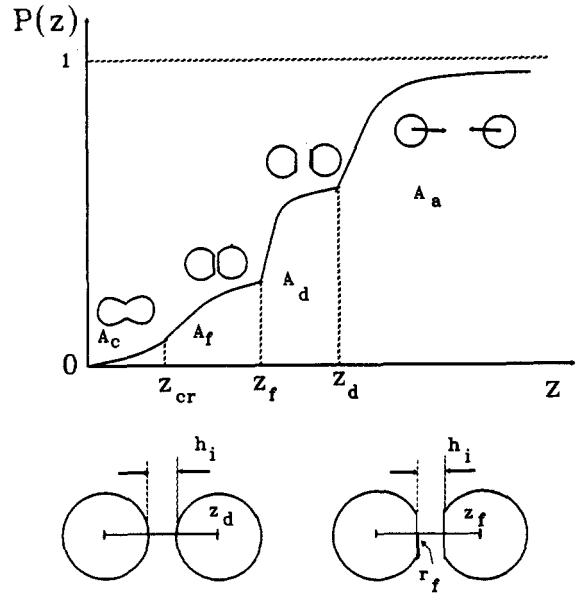

Figure 1. (a, top) Schematical presentation of the pair probability distribution function $P(z)$ for deformable coalescing droplets. z is the distance between the mass centers of the droplets. A_a denotes the region of nondeformed droplets approach, A_d denotes the region of droplet deformation, A_f denotes the region of film thinning, and A_c denotes the region of droplet fusion. z_d is the distance at which the deformation occurs, z_f is the distance at which the planar film thinning starts, and z_{cr} is the critical distance of film rupture. (b, bottom) Droplet configurations at the points z_d and z_f. h_i is the separation between the drop surfaces at which the deformation occurs and r_f is the film radius in the region A_f.

potential interaction energy $W(z)$. Let $P(z)$ be the probability to find another particle situated at a distance z from the central droplet (more precisely, z is the distance between the centers of mass of the particles). Similarly to the case of macroemulsions, the approach of the droplets is supposed to follow the scheme shown in Figure 1a.

At large distances, $z \to \infty$, the probability $P(z)$ tends to a constant value $P(z \to \infty) = 1$. The first stage (region A_a in Figure 1) presents the approach of two spherical or slightly deformed droplets of radius a. The distance z in this region adopts values between $z_d = 2a + h_i$ and infinity (h_i is the minimal distance between the droplet surfaces prior to the film formation). This region can be described by the theory of barrier diffusion of spherical particles.[8,10]

The second stage, below the distance z_d (see region A_d in Figure 1) represents rapid deformation of the droplet caps and formation of a flat film. This occurs at given value, h_i, of the minimal distance between the droplet surfaces; see Figure 1b. We will call h_i (the thickness at which the curvature at the droplet caps inverts its sign) *thickness of film formation*. In this stage the radius, r, of the formed plane-parallel film gradually (but rapidly[17,18]) changes from zero to a certain maximum value (denoted hereafter by r_f). Although the thickness of the film can be assumed to remain constant during this process, the distance between the *mass centers* changes (due to the deformation) from z_d to z_f.[15] It was shown analytically[17,18] and numerically[21] that the rate of film expansion is very high. For small (micrometer size) particles the plane-parallel film may appear without being preceded by dimple formation.[18]

During the third stage (region A_f in Figure 1) the film thins from thickness h_i to the critical thickness of rupture

(20) Danov, K. D.; Petsev, D. N.; Denkov, N. D.; Borwankar, R. *J. Chem. Phys.* Submitted for publication.

(21) Yiantsios, S. G.; Davis, R. H. *J. Colloid Interface Sci.* **1991**, *144*, 412.

h_{cr} at (almost) constant radius, r_f. The distance between the mass centers of the two droplets in the moment of rupture is z_{cr}. The rate of film thinning depends on different hydrodynamic and thermodynamic factors.[18,21-24] The thickness at which the film ruptures, h_{cr}, can be determined by using the simple formula derived by Vrij et al.[25] (see eq 3.23 below). A more general analysis[16] showed that quantitatively this formula gives good results despite of the assumptions made in the course of its derivation.

In the last stage, after the film rupture (region A_c in Figure 1), the mass centers of the droplets approach from z_{cr} to $z = 0$ and rapid fusion of the droplets is accomplished.

2.2. General Equations. We will confine ourselves to solving the stationary problem where the particle flux J, directed toward the central droplet is assumed to be constant (i.e. $\nabla \cdot \boldsymbol{J} = 0$)

$$J = 4\pi z^2 n_\infty D\left[\frac{dP}{dz} + P\frac{d}{dz}\left(\frac{W}{kT}\right)\right] = \text{const} \qquad (2.1)$$

where k is the Boltzmann constant, T is the temperature, n_∞ is the particle number density at $z \to \infty$, and $D(z)$ is the mutual diffusion coefficient. Equation 2.1 can be transformed into

$$\frac{J}{4\pi z^2 n_\infty D}\exp\left(\frac{W}{kT}\right) = \frac{d}{dz}\left[\exp\left(\frac{W}{kT}\right)P\right] \qquad (2.2)$$

Equation 2.2 describes the whole process depicted in Figure 1. The boundary conditions, necessary for its solution, can be chosen as follows:[3]

$$P \to 1,\ W \to 0 \qquad \text{at } z \to \infty \qquad (2.3)$$
$$P \to 0 \qquad \text{at } z \to 0$$

The probability function $P(z)$ is supposed to be continuous at the points z_{cr}, z_f, and z_d (see Figure 1). On integration of eq 2.2 along with the boundary conditions (2.3), the following expression for the flux J can be obtained:

$$J = J_{sm}/W_F \qquad (2.4)$$

where the Smoluchowski flux is defined as[1]

$$J_{sm} = 16\pi D_0 a n_\infty \qquad (2.5)$$

and W_F is the Fuchs factor accounting both for the hydrodynamic and the direct interactions between the droplets.[8,10] It is defined as

$$W_F = 4D_0 a\int_0^\infty \frac{1}{z^2 D(z)}\exp\left(\frac{W(z)}{kT}\right)dz \qquad (2.6)$$

The diffusion coefficient of a single droplet, D_0 can be expressed through the Stokes–Einstein formula

$$D_0 = \frac{kT}{6\pi\eta a} \qquad (2.7)$$

where η is the dynamic viscosity of the disperse medium. The mobility of the "central" droplet is taken into account in the Smoluchowski flux (eq 2.5).

The probability distribution $P(z)$ can be calculated by integrating eq 2.2 along with the boundary condition at $z \to \infty$ (2.3)

$$P(z) = \exp\left[-\frac{W(z)}{kT}\right]\left[1 - \frac{J}{4\pi n_\infty}\int_z^\infty \frac{1}{x^2 D(x)}\exp\left[\frac{W(x)}{kT}\right]dx\right] \qquad (2.8)$$

By combining eq 2.8 with eqs 2.4–2.7, one obtains

$$P(z) = \exp\left[-\frac{W(z)}{kT}\right]\left\{1 - \frac{\int_z^\infty \frac{1}{D(x)x^2}\exp\left[\frac{W(x)}{kT}\right]dx}{\int_0^\infty \frac{1}{D(x)x^2}\exp\left[\frac{W(x)}{kT}\right]dx}\right\} \qquad (2.9)$$

The probability function $P(z)$ given by eq 2.9 does not correspond to equilibrium. The exponential factor in the right-hand side of eq 2.9 is the equilibrium probability function (for diluted systems $W(z)$ has the meaning of a potential of mean force), while the term in the braces has a nonequilibrium (but steady) nature.

2.3. Determination of the Film Formation Thickness h_i. In order to find the distance, h_i, at which the deformation starts, we need to know the force acting on the particles during their approach (see the next subsection for more details). Equation 2.1 can be rewritten in the form

$$\frac{J\gamma(z)}{4\pi z^2 n_\infty P(z)} = kT\frac{d}{dz}[\ln P(z)] + \frac{dW(z)}{dz} \qquad (2.10)$$

where $\gamma(z)$ is the hydrodynamic resistance to the mutual droplet motion

$$\gamma(z) = \frac{kT}{D(z)} \qquad (2.11)$$

Let $V(z)$ be the mean droplet velocity of directional motion toward the central droplet. The flux J, the particle concentration $n_\infty P(z)$, and the velocity $V(z)$ are connected through the relationship

$$V(z) = \frac{J}{4\pi z^2 n_\infty P(z)} \qquad (2.12)$$

On the other hand, in the framework of the linear hydrodynamics, the droplet velocity is proportional to the applied force, i.e.

$$F_T(z) = \gamma(z)\, V(z) \qquad (2.13)$$

where $F_T(z)$ is the total drag force, acting between the droplets. From eqs 2.10, 2.12, and 2.13 one obtains

$$F_T(z) = kT\frac{d}{dz}[\ln P(z)] + \frac{dW(z)}{dz} \qquad (2.14)$$

We must emphasize that when deriving the expression (2.14) neither the type of the resistance $\gamma(z)$ nor the energy $W(z)$ was specified. Hence, as a general result we obtain that in the case of steady diffusion the total force acting on the droplet, F_T, is a superposition of the Brownian (diffusion) force (i.e. $kT\nabla[\ln P(z)]$) and the potential force which is due to direct interactions between the particles, $\nabla[W(z)]$. In this respect the situation is similar to the case of diffusion equilibrium in an external field considered long ago by Einstein.[26] As suggested by him the equilibrium is sustained by the counterbalance of the Brownian force (gradient of the particle concentration) and that due to the external field. Batchelor[27] applied this approach

(22) Chakarova, S. K.; Dupeyrat, M.; Nakache, E.; Dushkin, C. D.; and Ivanov, I. B. *J. Surf. Sci. Technol.* **1990**, *6*, 17.
(23) Ivanov, I. B.; Jain, R. K.; Somasundaran, P.; Traykov, T. T. In *Solution Behavior of Surfactants*; Mittal, K. L., Ed.; Plenum: New York, 1979; Vol. 2, p 817.
(24) Maldarelli, C.; Jain, R. K. In *Thin Liquid Films*; Ivanov, I. B., Ed.; Marcel Dekker: New York, 1988; p 497.
(25) Vrij, A.; Hesselink, F.; Lucassen, J.; van den Tempel, M. *Proc. K. Ned. Acad. Wet.* **1970**, *B73*, 124.
(26) Einstein, A. *Ann. Phys.* **1905**, *17*, 549.
(27) Batchelor, G. K. *J. Fluid Mech.* **1976**, *74*, 1.

to investigate the equilibrium in a system of interacting colloidal particles. In our notation $F_T(z) = 0$ at equilibrium. The system of coalescing droplets, however, is out of equilibrium and $F_T(z) \neq 0$. Equations 2.14 and 2.10 give

$$F_T(z) = \frac{J\gamma(z)}{4\pi z^2 n_\infty P(z)} \tag{2.15}$$

The calculation of the integral in eq 2.6 requires knowledge (i) of the distances z_f and z_{cr} at which the film formation and the film rupture take place (see subsection 2.1 and Figure 1) and (ii) of the explicit expressions for the interaction energy $W(z)$ and the mutual diffusivity $D(z)$. The film formation thickness h_i depends on the total force F_T[17,18]

$$h_i = \frac{F_T}{2\pi\sigma} \tag{2.16}$$

where σ is the interfacial tension. Equation 2.16 was derived[16-18] by assuming that the drag force F_T is constant. However, one can prove that it holds also for variable $F_T(z)$ if the particle motion is quasi-steady.[28] From eqs 2.15 and 2.16 one obtains

$$h_i = \frac{J\gamma(z_d)}{8\pi^2\sigma z_d^2 n_\infty P_d} \tag{2.17}$$

with P_d being the probability function at $z = z_d$ (see Figure 1). Integrating eq 2.2, along with the boundary condition at $z = 0$ (eq 2.3), we find the probability P_d (cf. also eq 2.11)

$$P_d = \frac{J}{4\pi n_\infty kT}\int_0^{z_d}\frac{\gamma(z)}{z^2}\exp\left[\frac{W(z) - W(z_d)}{kT}\right]dz \tag{2.18}$$

Introducing eq 2.18 into eq 2.17 leads to a transcendental equation for determination of h_i (recall that $z_d = h_i + 2a$)

$$h_i = \frac{kT}{2\pi\sigma z_d f} \tag{2.19}$$

with f, defined by the following expression:

$$f = \int_0^{z_d}\left(\frac{z_d}{z}\right)^2\frac{\gamma(z)}{\gamma(z_d)}\exp\left[\frac{W(z) - W(z_d)}{kT}\right]\frac{dz}{z_d} \tag{2.20}$$

The integral in eq 2.20 must be evaluated over three regions: A_c, A_f, and A_d. It is reasonable to assume that the contribution from region A_c is much smaller than the ones from the other two regions, A_f and A_d. This assumption is supported by the following facts: (i) the film rupture and particle fusion are accompanied with sharp decrease in the surface energy of the droplets and, hence, in this region $W \ll W_d$ and the exponent in the integral in eq 2.20 is very small; (ii) the rate of coalescence is much greater than the rate of film thinning, especially when surfactants are present (this means that the ratio $\gamma(z)/\gamma(z_d)$ in the same integral is much less than unity in the region A_c). Hence, the integral over the region A_c is negligible in comparison with those over A_f and A_d. An additional possibility for simplification is suggested by the results of the numerical calculations which show that $h_i \ll a$.[16,18] Hence, with sufficient accuracy one can replace z/z_d by $z/2a$. As a result, eqs 2.19 and 2.20 can be simplified to read

$$h_i = \frac{kT}{4\pi\sigma a f_0},$$

$$f_0 = \int_{z_{cr}}^{z_d}\left(\frac{2a}{z}\right)^2\frac{\gamma(z)}{\gamma(z_d)}\exp\left(\frac{W(z) - W(z_d)}{kT}\right)\frac{dz}{2a} \tag{2.21}$$

This equation allows calculation of h_i if $\gamma(z)$, $W(z)$, and z_{cr} are known. Equation 2.21 should be solved numerically because of the complex relation between $h_{cr} = z_{cr} - 2a$ and h_i[18,22,24,25] (see eq 3.23 below).

After the determination of h_{cr} (e.g. from eq 3.23) and h_i one can obtain the factor W_F (cf. eq 2.6). By using eq 2.4, the diffusion flux J can be calculated, which is directly related to the coalescence rate. For example, the rate of droplet coalescence in the beginning of the process is[1]

$$dn_2/dt = k_c n_\infty^2 \tag{2.22}$$

where n_2 is the concentration of larger droplets formed by coalescence of two droplets of radius a and k_c is the respective rate constant given by the expression

$$k_c = \frac{J}{n_\infty} = \frac{16\pi D_0 a}{W_F} \tag{2.23}$$

If we are interested in the further evolution of the system, when even larger droplets are formed, we should develop a kinetic scheme similar to that developed by Smoluchowski for the coagulation of aggregates of solid particles.[1] Such analysis will be presented in a subsequent paper.

3. Potential and Hydrodynamic Interactions between Two Approaching Deformable Droplets

To make use of the general expressions derived above, one must specify the functions $W(z)$ and $\gamma(z)$ for the system under consideration.

The potential energy of interaction between two deformable droplets can be written as a sum of several terms[15,20]

$$W = W^S + W^{VW} + W^E + \Delta W \tag{3.1}$$

where W^S is the change of the surface energy due to droplet deformation, W^{VW} is the van der Waals term, W^E is the electrostatic energy of interaction, and ΔW stands for other possible interactions (e.g. steric, structural, etc.[10,29]). These contributions are specified below.

3.1. Surface Deformation Energy. During the process of approach the droplet volume remains constant. The change of the interfacial energy is due to the fact that any deviation of the droplet shape from the spherical one (at constant volume) is accompanied with an increase in the interfacial area. This leads to a corresponding increase in the free energy of the system.[15] Figure 2 illustrates the geometrical parameters of the deformed droplets in the model: a_s is the radius of the spherical part and l is the distance between the forepoint and the most remote point in a deformed droplet. The radius of the film during the stage of film thinning, r_f, can be expressed by the relationship (see eqs 294 and 296 in ref 18): $r_f^2 = ah_i$. Hence, during the stage of droplet deformation, region A_d in Figure 1, the film radius (denoted by r) *gradually increases* from 0 to the *final value*, $r_f = (ah_i)^{1/2} \ll a$. This means that for the system under consideration the deformation is small ($r/a \ll 1$) and with sufficient accuracy we can use the expression[15,20]

(28) Danov, K. D.; Velev, O. D.; Ivanov, I. B.; Borwankar, R. To be submitted for publication.

(29) Napper, D. H. *Polymeric Stabilization of Colloidal Dispersions*; Academic Press: New York, 1983.

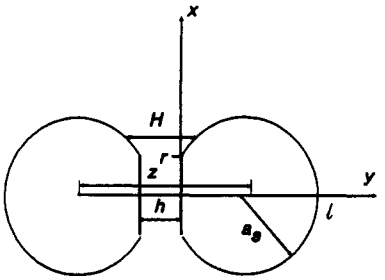

Figure 2. Model of two deformed emulsion droplets having the shape of spherical segments of radius a_s. r and h are the radius and the thickness of the film between the droplets.

$$\frac{1}{2}W^S = \sigma(S - S_0) + \frac{1}{2}E_G S_0[(S - S_0)/S_0]^2 \qquad (3.2)$$

where $S_0 = 4\pi a^2$ denotes the area of the nondeformed droplet and S is the total area of the deformed one and E_G is the effective Gibbs elasticity of the surfactant monolayer covering the droplet surface. The first term in the right-hand side of eq 3.2 accounts for the extension of the droplet surface at constant interfacial tension σ, while the second one is related to the possible increase in the interfacial tension during the deformation, caused by the stretching of the surfactant layer. The latter effect exists only if the surfactant transport onto the interface is slow (or absent) and cannot maintain the equilibrium adsorption at the droplet surface during the process of deformation. As discussed previously[15] this is probably the case of water-in-oil microemulsions when the surfactant is soluble in the disperse phase as well as the case of droplets covered with adsorbed layer of polymers or proteins. It can be shown that for $(r/a)^2 \ll 1$ (see Figure 2)

$$l = 2a\left[1 - \frac{1}{4}\epsilon^2 + 0(\epsilon^6)\right], \qquad a_s = a\left(1 + \frac{1}{16}\epsilon^4 + 0(\epsilon^6)\right] \qquad (3.3)$$

where $\epsilon = r/a \ll 1$. Equation 3.3 and the exact formula for S lead to[15,20]

$$S - S_0 = \pi r^2 + 2\pi a_s l - 4\pi a^2 = \pi a^2\left[\frac{1}{4}\epsilon^4 + 0(\epsilon^6)\right] \qquad (3.4)$$

Equations 3.2 and 3.4 show that the ratio of the second toward the first term in the right-hand side of eq 3.2 is $E_G\epsilon^4/(32\sigma)$. Hence Gibbs elasticity can be neglected for emulsions, where E_G and σ are comparable in magnitude. Therefore with sufficient accuracy

$$W^S = \frac{\pi\sigma r^4}{2a^2}, \qquad r \le r_f \ll a, \qquad \sigma \sim E_G \qquad (3.5)$$

In the case of microemulsions σ can be orders of magnitude lower than E_G and the second term could be important.[15] Hence, one should use the complete expression (3.2), which for $\epsilon \ll 1$ can be rewritten as

$$W^S = \frac{\pi\sigma r^4}{2a^2} + E_G\frac{\pi a^2}{64}\frac{r^8}{a_8} \qquad (3.6)$$

$$r \le r_f \ll a$$

3.2. Van der Waals Energy of Interaction. In ref 20 an exact formula for the van der Waals energy of interaction between the two deformed droplets, shown in Figure 2, was derived. For the particular case of small deformations (i.e. $r^2/a^2 \ll 1$) the exact expression can be simplified to read (for notations see Figure 2)

$$W^{VW} = -\frac{A_H}{12}\left[\frac{4a_s^2}{(2a_s + h)^2} + \frac{4a_s^2}{h(4a_s + h)} + 2\ln\left[\frac{h(4a_s + h)}{(2a_s + h)^2}\right] + \frac{128a_s^5 r^2}{h^2(2a_s + h)^3(4a_s + h)^2}\right], \qquad r \ll a \qquad (3.7)$$

where A_H is the Hamaker constant.[30] For $h \ll 2a$ eqs 3.3 and 3.7 lead to even simpler result

$$W^{VW} = -\frac{A_H}{12}\left[\frac{a}{h} + 2\ln\left(\frac{h}{a}\right) + \frac{3}{4} + \frac{r^2}{h^2}\right] \qquad (3.8)$$

$$h \ll a, \qquad r \ll a$$

The first three terms in the brackets of eq 3.8 correspond to interaction between two nondeformed spherical droplets of radius a at gap width $h \ll a$, while the last term accounts for the presence of a planar film of thickness h in the deformed state.

In the region A_s (see Figure 1a) the exact Hamaker expression for the interaction between two spheres[30] should be used.

3.3. Electrostatic Interaction. In the case of oil-in-water emulsions the electrostatic energy of interaction should be taken into account as well. For nondeformed (spherical) droplets one can use the potential of mean force derived by Beresford-Smith et al.[31]

$$W^E = \frac{kT}{\lambda}a^2 y_s^2\frac{\exp(-\kappa h)}{z} \qquad (3.9)$$

where λ is the so-called Bjerrum length and κ is the inverse Debye screening length (for simplicity only the presence of 1:1 electrolyte is considered)

$$\lambda = \frac{e^2}{\mathcal{E}kT} \approx 0.7 \text{ nm, at } T = 298\ K \qquad (3.10)$$

$$\kappa^2 = 8\pi\lambda C_{el} \qquad (3.11)$$

e is the elementary charge, $\mathcal{E}$ is the dielectric constant of the disperse medium, and C_{el} is the electrolyte number concentration. The dimensionless quantity y_s in eq 3.9 is related to the surface potential (or charge density) of the droplets and can be determined by numerical integration of the nonlinear Poisson–Boltzmann equation.[31-33] In the case of low surface potentials ($\Psi_s < 25$ mV), y_s can be approximated by the dimensionless surface potential

$$y_s \approx \frac{e\Psi_s}{kT}, \qquad \text{for } \Psi_s < 25 \text{ mV} \qquad (3.12)$$

In miniemulsions a is typically between 0.1 and 10 μm. For electrolyte concentration higher than 10^{-3} M (1:1 electrolyte) the product κa is much greater than unity and the electrostatic interaction between the droplets takes place only at small gap widths ($\kappa h \sim 1$, $h \ll a$). In this case one can use for the electrostatic energy of interaction between two *deformed droplets* the approximate expression[20]

$$W^E = \frac{kT}{2\lambda}y_s^2 a\exp(-\kappa h)\left[1 + (\kappa a)\frac{r^2}{a^2}\right] \qquad (3.13)$$

$$r \ll a, \qquad \kappa a \gg 1$$

(30) Hamaker, H. C. *Physica* **1937**, *4*, 1058.
(31) Beresford-Smith, B.; Chan, D. Y. C.; Mitchell, D. J. *J. Colloid Interface Sci.* **1985**, *105*, 216.
(32) Alexander, S.; Chaikin, P. M.; Grant, P.; Morales, G. J.; Pincus, P. *J. Chem. Phys.* **1984**, *80*, 5776.
(33) Denkov, N. D.; Petsev, D. N. *Physica A* **1992**, *183*, 462.

The unity in the brackets in eq 3.13 corresponds to the interaction between two charged spheres for $h \ll a$ (cf. with eq 3.9) and the second term is due to the deformation. This expression is used in the numerical calculations below. Besides, for $\kappa a \gg 1$ one can express analytically the parameter y_s for arbitrary surface potential, Ψ_s, by using eqs 14 and 15 in the paper of Chew and Sen[34] and eq 4.35 in the work of Beresford-Smith et al.[31]

3.4. Hydrodynamic Resistance for Two Deformed Droplets Approaching Each Other. By equating the dissipated energy to the work of the outer forces, Charles and Mason[35] obtained the following expression for the hydrodynamic resistance of two approaching solid particles at small distances (i.e. in lubrication approximation)

$$\gamma = 6\pi\eta\int_0^\infty \left(\frac{x}{H}\right)^3 dx \tag{3.14}$$

where x is the radial coordinate (see Figure 2) and $H = H(x)$ is the local thickness of the gap, between the particle surfaces. For solid spheres this yields Taylor's result $\gamma = 6\pi\eta a^2/h$. However, it was shown[17] that this approach is not applicable when droplets or bubbles with tangentially mobile surfaces are considered. In such cases one can proceed in the following way. The force acting on one of the droplets is[18] (see Figure 2)

$$F_T = -\pi\int_0^\infty x^2\left(\frac{\partial P_s}{\partial x}\right) dx \tag{3.15}$$

where P_s is the scalar pressure at the surface of the droplet (eq 3.15 holds for particles of arbitrary shape). It is related to the thinning velocity V and the radial component of the velocity U at the droplet surface by means of the expression, following from lubrication theory[18]

$$\frac{\partial P_s}{\partial x} = -6\frac{V\eta}{H^3}x + 12\frac{U\eta}{H^2} \tag{3.16}$$

For a system of two deformed droplets like those shown in Figure 2, the distance between the particle surfaces $H(x)$ can be assumed with sufficient accuracy to be:

$$H = h \quad \text{for} \quad x \le r \tag{3.17}$$
$$H = h - \frac{r^2}{a} + \frac{x^2}{a} \quad \text{for} \quad x > r$$

The radial component of the velocity U can be expressed as[18]

$$U = \frac{Vx}{2H(1+\epsilon^e+\epsilon^f)} \quad \text{for} \quad x \le r \tag{3.18}$$

The quantities ϵ^e and ϵ^f account for the surfactant diffusivity in the disperse phase and/or media, as well as for the droplet surface properties and can vary within a wide range of values.[16-18] The effect of the surface viscosity is neglected in eq 3.18 but in principle it can be taken into account. We are not aware of a theory giving a complete description of the fluid motion in the meniscus region when surfactants are present. For that reason we use the fact that when the local spacing between the droplet surfaces increases (see eq 3.17), the radial component of the velocity decreases. Hence, the surface mobility is important only in the film and in a narrow region surrounding it. In order to account (although approximately) for the hydrodynamic resistance of the meniscus region around the film, we suppose that in this region the surface mobility is absent, i.e. $U = 0$ for $x > r$. Introducing eqs 3.16–3.18 into eq 3.15 and performing the integration we obtain (see also eq 2.13)

$$\gamma = 6\pi\eta\left[\int_0^r \frac{\epsilon^e+\epsilon^f}{1+\epsilon^e+\epsilon^f}\left(\frac{x}{H}\right)^3 dx + \int_r^\infty \left(\frac{x}{H}\right)^3 dx\right]$$
$$= \frac{3\pi\eta a^2}{2h}\left(\epsilon_s + \frac{r^2}{ah} + \frac{r^4}{a^2h^2}\right) \tag{3.19}$$

where ϵ_s denotes an average value of the ratio $(\epsilon^e+\epsilon^f)/(1+\epsilon^e+\epsilon^f)$ and can acquire values between 1 (for tangentially immobile surfaces) and 0.001 (for pure liquids or when the surfactant is soluble only in the droplet phase). Typical values of ϵ_s for systems with surfactants soluble only in the continuous phase are between 0.1 and 1; for systems with surfactants soluble only in the emulsion droplets ϵ_s is between 0.001 and 0.01.[36,37]

Combining eqs 2.21, 3.6, 3.8, 3.13, and 3.19, and taking into account that[18] $r_f^2 = ah_i$, we can transform the transcendental equation for h_i in the form

$$h_i = \frac{kT}{2\pi\sigma(f_d+f_f)}\epsilon_s \tag{3.20}$$

where the dimensionless factor f_d accounts for the influence of the region of deformation A_d. It is given by the expression

$$f_d = \int_0^1 (1+\bar{r}+\bar{r}^2)\exp\left(\frac{\pi\sigma h_i}{2kT}\left[\bar{r}^2 + \frac{E_G h_i}{32a^2\sigma}\bar{r}^4 - \frac{A_H a}{6\pi\sigma h_i^3}\bar{r} + \frac{kTy_s^2(\kappa a)^2}{2\pi\sigma\lambda a}\exp(-\kappa h_i)\bar{r}^2\right]\right) d\bar{r} \tag{3.21}$$

where $\bar{r} = r/r_f$ is the dimensionless film radius.

The other dimensionless factor f_f accounts for the contribution of the film thinning region A_f and is given by

$$f_f = \exp\left(\frac{\pi\sigma h_i^2}{2kT} + E_G\frac{\pi h_i^4}{64a^2kT}\right)\int_{\bar{h}_{cr}}^1 \left(1+\frac{1}{\bar{h}}+\frac{1}{\bar{h}^2}\right)\times \left(\frac{1}{\bar{h}}\right)^{1+(A_H/6kT)} \exp\left[\frac{A_H a}{12kTh_i}\left(1-\frac{1}{\bar{h}}-\frac{1}{\bar{h}^2}\right) + \frac{y_s^2 a}{2\lambda}\left(1+\frac{\kappa^2 h_i^2}{2}\right)\exp(-\kappa h_i\bar{h}) - \frac{y_s^2 a}{2\lambda}\exp(-\kappa h_i)\right] d\bar{h} \tag{3.22}$$

with $\bar{h} = h/h_i$ being the dimensionless film thickness and $\bar{h}_{cr}$ denotes the ratio h_{cr}/h_i. For the numerical calculations presented below, the latter is evaluated using the approximate formula of Vrij,[25] which can be transformed to read:

$$\bar{h}_{cr} = h_{cr}/h_i = 0.243\left(\frac{A_H^2 a^2}{2\pi\sigma^2 h_i^6}\right)^{1/7} \tag{3.23}$$

Although this formula was derived under strong restrictions (e.g., for tangentially immobile surfaces and only van der Waals attraction present), the calculations showed that the value of h_i is very weakly dependent on $\bar{h}_{cr}$ for the parameters we used. If necessary one can apply more complete (and complex) expressions for the determination of h_{cr}.[16,24,38]

4. Numerical Results and Discussion

In this section numerically calculated values of the thickness h_i, at which the droplet deformation takes place

(34) Chew, W. C.; Sen, P. N. *J. Chem. Phys.* **1982**, *77*, 2042.
(35) Charles, G. E.; Mason, S. G. *J. Colloid Sci.* **1960**, *15*, 236.
(36) Traykov, T. T.; Ivanov, I. B. *Int. J. Multiphase Flow* **1977**, *3*, 471.
(37) Traykov, T. T.; Manev, E. D.; Ivanov, I. B. *Int. J. Multiphase Flow* **1977**, *3*, 485.
(38) Maldarelli, C.; Jain, R. K.; Ivanov, I. B.; Ruckenstein, E. *J. Colloid Interface Sci.* **1980**, *78*, 118.

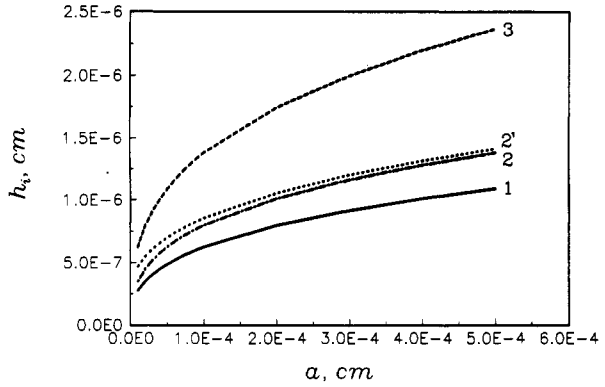

Figure 3. Dependence of the distance of droplet deformation h_i on the droplet radius a: $A_H = 5 \times 10^{-21}$ J and $\epsilon_s = 0.1$ (curve 1); $A_H = 1 \times 10^{-20}$ J and $\epsilon_s = 0.1$ (curve 2); $A_H = 5 \times 10^{-20}$ J and $\epsilon_s = 0.1$ (curve 3); $A_H = 1 \times 10^{-20}$ J and $\epsilon_s = 0.001$ (curve 2'). The interfacial tension is $\sigma = 1$ mN/m for all curves.

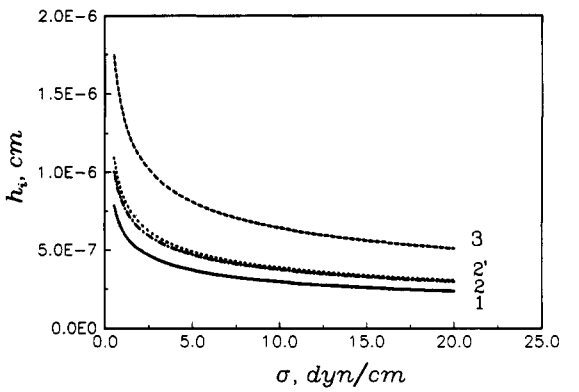

Figure 4. Dependence of the distance of droplet deformation, h_i, on the interfacial tension σ: $A_H = 5 \times 10^{-21}$ J and $\epsilon_s = 0.1$ (curve 1); $A_H = 1 \times 10^{-20}$ J and $\epsilon_s = 0.1$ (curve 2); $A_H = 5 \times 10^{-20}$ J and $\epsilon_s = 0.1$ (curve 3); $A_H = 1 \times 10^{-20}$ J and $\epsilon_s = 0.001$ (curve 2'). The droplet radius is $a = 1$ μm for all curves.

and of Fuchs factor W_F (see eq 2.6) are presented. The effects of different factors on h_i and W_F are examined.

4.1. Film Formation Thickness. Figure 3 shows the dependence of h_i on the droplet radius, a, for different values of the Hamaker constant, A_H (see eqs 3.20–3.22): $A_H = 5 \times 10^{-21}$ J (curve 1), $A_H = 1 \times 10^{-20}$ J (curves 2 and 2'), and $A_H = 5 \times 10^{-20}$ J (curve 3). The used values of A_H are within the range accepted in the literature as typical for oil and water emulsions.[15,19,39] The interfacial tension was assumed to be $\sigma = 1$ mN/m for all these curves. Electrostatic interactions are not included when calculating these data. Curves 1–3 were calculated with $\epsilon_s = 0.1$, which is considered to be a typical value for emulsions, stabilized with surfactant soluble in the continuous phase.[18,37] For curve 2' all parameters are the same as for curve 2 except for ϵ_s, which is now 0.001. The latter value corresponds to systems without surfactants, to systems containing surfactant only in the droplet phase, or to emulsions containing mixture of surfactants with at least one of them being in the droplets (e.g. when a demulsifier is present).

From Figure 3 one sees that for micrometer size droplets h_i is between 5 and 25 nm and slightly depends on the droplet radius. For particles smaller than 1 μm, one observes a significant decrease in h_i. This region is investigated in more detail below, when the deformability of *microemulsion* droplets is briefly discussed. On the other hand, h_i depends on the Hamaker constant: the stronger the attraction, the larger h_i. The plotted values for h_i seem quite reasonable and show that the Brownian force may lead to deformation of the emulsion droplets and formation of planar films during the collisions between them. It is interesting to note that the enhanced tangential mobility of the droplet interfaces, which strongly affects the rate of film thinning (and hence the film lifetime[18,21-23]) practically does not change h_i; cf. curves 2 and 2' which differ only in the value of ϵ_s used. This means that the increased tangential mobility of the interfaces shortens the time of film drainage but does not change the distance at which the droplet deformation starts. This result is in accordance with the theoretical prediction made by Ivanov et al.[17] that the shape of deformable approaching droplets depends mainly on thermodynamics factors rather than on hydrodynamic ones.

In Figure 4 the effect of the interfacial tension, σ, on h_i is studied. The radius of the droplet is chosen to be $a = 1$ μm and the other parameters are the same as in Figure 3 ($A_H = 1 \times 10^{-20}$ J for curves 2 and 2', $A_H = 5 \times 10^{-21}$ J and $A_H = 5 \times 10^{-20}$ J for curves 1 and 3, respectively; $\epsilon_s = 0.1$ for curves 1 to 3 and $\epsilon_s = 0.001$ for curve 2'). One sees that h_i increases when σ decreases. At σ below 1 mN/m, sharp increase in h_i, is observed. Again, the increase in A_H leads to increase in h_i while ϵ_s almost does not affect the latter. These results are in agreement with the idea of Hofman and Stein[19] that lower interfacial tension may enhance the droplet deformation, thus affecting the emulsion stability.

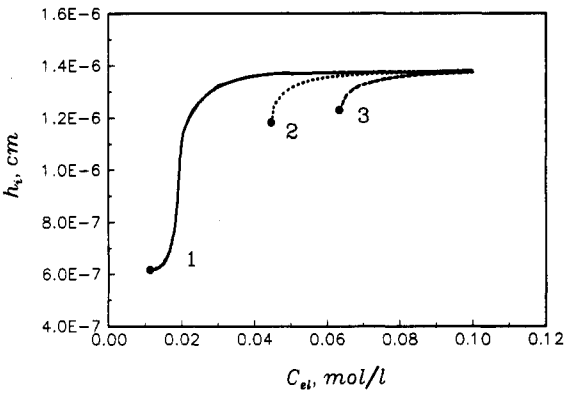

Figure 5. Influence of the electrolyte concentration, C_{el}, on the deformation distance h_i: $\Psi_s = 50$ mV (curve 1); $\Psi_s = 25$ mV (curve 2); $\Psi_s = 10$ mV (curve 3). $A_H = 10^{-20}$ J, $a = 5$ μm, $\sigma = 1$ mN/m, and $\epsilon_s = 0.1$ for all curves. The full points at the ends of the curves correspond to concentrations, where the droplet deformation becomes improbable.

The influence of the electrostatic repulsion on h_i, in the case of oil-in-water emulsions, is demonstrated in Figure 5. The plotted curves represent the dependence of h_i on the electrolyte concentration, C_{el}, for three different surface potentials: 50 mV (curve 1), 25 mV (curve 2), and 10 mV (curve 3). The other parameters are, $\sigma = 1.0$ mN/m, $a = 5$ μm, $A_H = 1 \times 10^{-20}$ J, and $\epsilon_s = 0.1$. It turns out (see Figure 5) that at a given surface potential the electrostatic repulsion reduces very slightly h_i above a certain electrolyte concentration. At high ionic strengths (e.g. $C_{el} > 0.08$ M for the potentials used in these calculations) the effect of the electrostatic interactions on h_i can be entirely neglected. Obviously, this is not true when considering the hydrodynamic drainage and rupture of the formed film, where the electrostatic contribution in the disjoining pressure should be taken into account. However, below some critical ionic strength the physically reasonable root of eq 3.20 (which determines the value of h_i) disappears; see the points at the ends of the curves. This means, that

(39) Visser, J. *Adv. Colloid Interface Sci.* **1972**, *3*, 331.

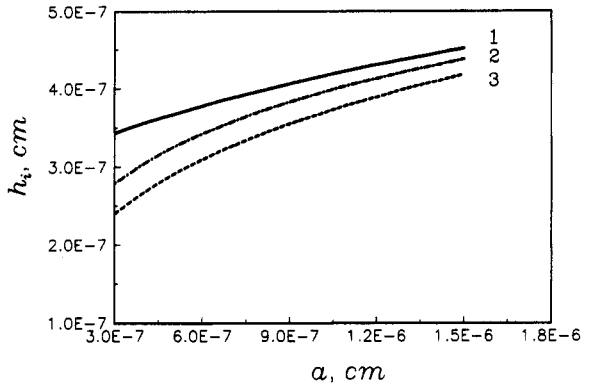

Figure 6. Deformation distance, h_i, vs the droplet radius, a, in microemulsion systems: $\sigma = 0.1$ mN/m, $A_H = 10^{-20}$ J, $\epsilon_s = 0.1$, $E_G = 0$ (curve 1), $E_G = 10$ mN/m (curve 2), $E_G = 30$ mN/m (curve 3).

below this electrolyte concentration the electrostatic repulsion prevents the particles from deformation and film formation. In other words, the kinetic energy of the droplets is not large enough to overcome the energy barrier accompanying the droplet deformation and the particles behave as nondeformable charged spheres. This point deserves additional theoretical and experimental investigation in the future, because such a qualitative change in the trend of the occurring processes may be related to a drastic change in the emulsion stability. In particular, the strong dependence of the emulsion stability on the electrolyte concentration measured by Hofman and Stein[19] (see their Figures 1 and 2), may stem from this effect.

We dealt above mostly with micrometer size droplets, which are typical for common *miniemulsions*. However, similar considerations apply to *microemulsion* systems (nanometer size droplets) as well. It has been shown that collisions between microemulsion droplets may lead to coalescence of the colliding droplets and fusion of their cores[40] in the case of four-component microemulsion systems. It was argued[15] that this and other observations of the behavior of microemulsions can be explained by assuming that a planar film forms during collision between the droplets before they coalesce or rebounce. We will discuss now this problem in the framework of the present theory. The curves in Figure 6 show h_i as a function of the droplet radius a, at some typical parameters for microemulsions (see also the discussion on pp 164–165 in ref 15): $\sigma = 0.1$ mN/m, $A_H = 1 \times 10^{-20}$ J, $\epsilon_s = 0.1$. As discussed previously[15] the Gibbs elasticity, E_G, should be accounted for when considering the deformation energy in the case of microemulsions because the interfacial tension is very low in these systems, $\sigma \ll E_G$ (see also eq 3.6 above). The three curves in Figure 6 correspond to different values of E_G: $E_G = 0$ (curve 1), $E_G = 10$ mN/m (curve 2), and $E_G = 30$ mN/m (curve 3). One sees that h_i is about 2 to 5 nm and slightly decreases with E_G. The calculated figures are quite reasonable for these systems (note, that $a \sim 10$ nm in this case). Besides, the results confirm the rough estimates based on a rather different approach[15]—namely, by comparison of the kinetic energy with the potential interaction energy between the droplets. Still the calculations for microemulsions are mainly illustrative because a more complete consideration should include some other effects (e.g. bending elasticity and spontaneous curvature) as well. The use of the simple eq 3.23 for calculation of h_{cr} is also questionable for such small droplets.

(40) Lang, J.; Lalem, N.; Zana, R. *J. Phys. Chem.* **1991**, *95*, 9533.

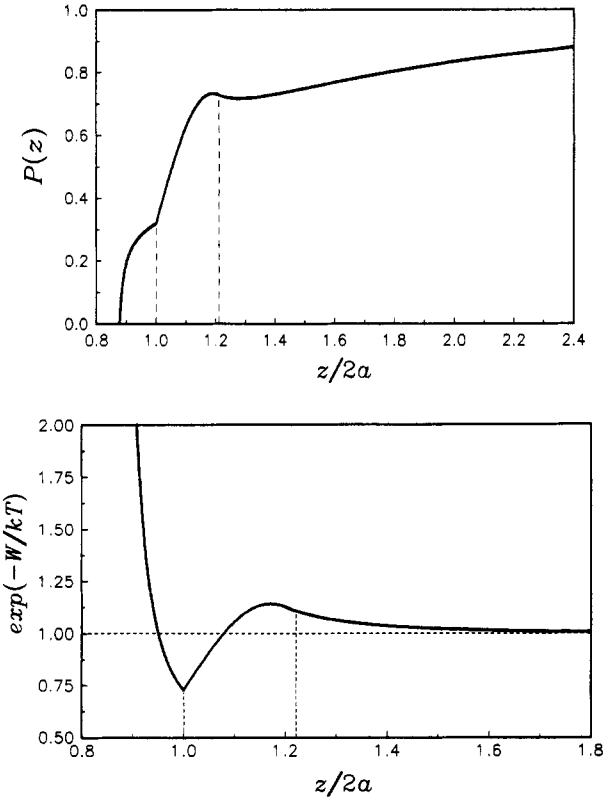

Figure 7. (a, top) Pair probability function $P(z)$ for microemulsions (see eq 2.9). The parameters used are $a = 10$ nm, $\sigma = 0.1$ mN/m, $A_H = 10^{-20}$ J, $\epsilon_s = 0.1$, and $E_G = 0$. The vertical dashed lines denote the onset and the end of the droplet deformation (film formation). (b, bottom) Plot of $\exp(-W(z)/kT)$ for the same system.

4.2. Radial Distribution Function. In Figure 7a, the nonequilibrium steady pair probability function $P(z)$ is presented (cf. the illustrative scheme shown in Figure 1). The parameters used are: $a = 10$ nm, $\sigma = 0.1$ mN/m, $E_G = 0$, $A_H = 10^{-20}$ J, $\epsilon_s = 0.1$ (cf. curve 1 in Figure 6). It is seen that $P(z)$ is always less than 1, due to the imposed boundary condition (2.3) used when solving eq 2.1 and leading to the flux term in eq 2.9. The dashed lines indicate the starting and final stages of the droplet deformation. For comparison the function $\exp(-W(z)/kT)$ is plotted in Figure 7b for the same system. It is seen that both curves are quite different, which is due to the nonequilibrium term in eq 2.9.

4.3. Fuchs' Factor. The effect of the droplet deformability on the coalescing rate can be evaluated by calculating Fuchs' factor W_F; see eq 2.6. For comparison, one can use Fuchs' factor for the coagulation of nondeformable spheres of the same size, Hamaker constant, and, eventually, electrical surface potential. In Figure 8 W_F vs a is plotted for microemulsion droplets. The parameters for these calculations are $A_H = 1 \times 10^{-20}$ J, $\sigma = 0.1$ mN/m, and $\epsilon_s = 1$. The different curves correspond to different Gibbs elasticities of the surfactant monolayer: $E_G = 0$ (curve 1), $E_G = 10$ (curve 2), and $E_G = 30$ (curve 3). The electrostatic interaction is ignored in these calculations. The horizontal dashed line 4 is for nondeformed spheres with tangentially immobile surfaces and the same A_H, initial radius a, etc. One sees that for such small droplets the deformability leads to an increase of W_F in comparison with its value for hard spheres, i.e. to a decrease of the coalescence rate. The effect is slightly dependent on E_G and disappears with the increase of the droplet size. The dotted line 5 is for two nondeformable spheres with tangentially mobile surfaces (bubbles in the absence of surfactant). The rate

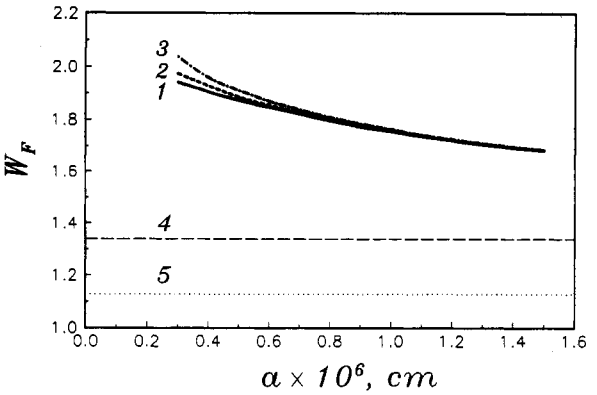

Figure 8. Dependence of the efficiency factor W_F (cf. eqs 2.4 and 2.6) on the droplet radius, a, for microemulsion systems. The parameters are the same as in Figure 6. The dashed line 4 corresponds to the coagulation of hard spheres with $A_H = 10^{-20}$ J. The dotted line 5 is for spherical bubbles with tangentially mobile surfaces.

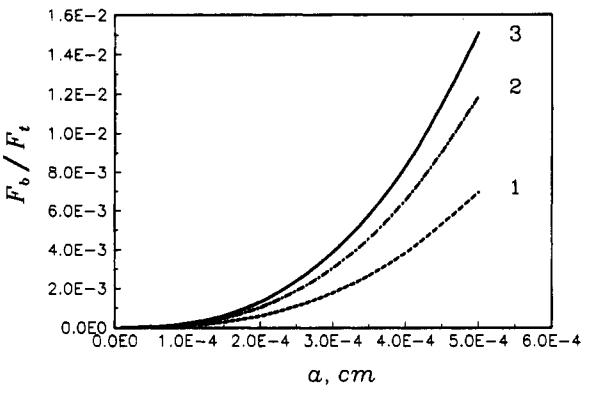

Figure 9. Ratio of the buoyancy force, F_b (cf. eq 4.1) and the total force acting between the droplets (eq 2.14) vs the droplet radius a: $A_H = 5 \times 10^{-21}$ J (curve 1); $A_H = 10^{-20}$ J (curve 2); $A_H = 5 \times 10^{-20}$ J (curve 3). $\epsilon_s = 0.1$ for all curves.

of the two bubbles was calculated by using the theory of Haber et al.[41] The fact that W_f for deformable microemulsion droplets is greater than that for nondeformable spheres with tangentially immobile surfaces, while for bubbles it is smaller, means that the most important effect is due to the deformability of the particles. The tangential mobility is less important.

The numerical calculations show that W_F for deformable and nondeformable spheres of *micrometer size* practically coincide. This result means that for miniemulsions the mutual approach of the droplets prior to their deformation is the rate-determining stage in the considered coalescing scheme. That is why the coalescence rate is the same as for the coagulation of nondeformable spheres; see eq 2.23. The reason for that is mainly the high hydrodynamic resistance of mutual approach of the spherical droplets and large average interparticle distance. However, at large droplet concentrations (when eqs 2.22 and 2.23 are no longer valid) the coalescence kinetics cannot be investigated simply by considering Fuchs' factor. For example van den Tempel[42] showed that at high concentration, the long time kinetics is characterized by the parameter $k_{fl}n_\infty/k_{cl}$, where k_{fl} is the rate constant for droplet aggregation and k_{cl} is the rate constant for droplet coalescence inside an aggregate. In the terms of our consideration k_{fl} is connected with the mutual approach of nondeformed droplets, while k_{cl} is related to film thinning and rupture. Therefore, for more concentrated emulsions, the droplet deformability can be a substantial factor. Such an analysis will be published elsewhere.[43]

4.4. Importance of the Brownian and Intermolecular Forces. One question that can be raised is whether or not one can neglect the gravitational effects in the above treatment. To answer this question we calculated the force acting between the particles, F_T (including the Brownian force), at the distance of film formation, h_i, by using eq 2.15. In Figure 9 the ratio between the buoyancy force

$$F_b = \Delta\rho g \frac{4}{3}\pi a^3 \qquad (4.1)$$

and F_T, as a function of the droplet radius, is plotted. The curves correspond to different values of the Hamaker constant (the same as in Figure 1), $\sigma = 1$ mN/m, $\epsilon_s = 0.1$, and the mass density difference $\Delta\rho = 0.2$ g/cm^3. One sees that for droplets smaller than 10 μm in diameter, the ratio $F_b/F_T \leq 10^{-2}$. This means that for such particles the gravitation can be entirely neglected in comparison with the Brownian and surface forces when considering the mutual approach of the droplets in a homogeneous suspension. Moreover, if we assume that only the gravity force is operative (i.e. if we neglect the Brownian and direct forces in F_T) the substitution from eq 4.1 into eq 2.16 shows that for micrometer size droplets h_i should be below 0.1 nm. The latter value is unrealistic which means that the gravity alone cannot lead to droplet deformation in miniemulsions. Hence, the deformation predicted by our theory is essentially due to the incorporation of the Brownian and direct forces in the model. This conclusion is of great importance for the consideration of the coalescence in miniemulsions, since the coalescence stages and processes are different for systems of deformable and nondeformable droplets. On the other hand, due to gravity the micrometer size particles can slowly sediment (or float up) with time, thus leading to nonuniform spatial distribution of the droplets. This effect becomes even more pronounced with time, because the droplet coalescence increases the mean particle diameter. Hence, if we are interested in the overall lifetime of the emulsion, a more complete and refined consideration accounting for the sedimentation should be carried out.

Another force which can be important for the emulsion stability is the hydrodynamic force in shear[44] or in turbulent flows. An attempt for such considering the case of turbulence was performed by Kumar et al.[45]

4.5. Comparison with the Hofman and Stein Approach.[19] At the end of this section, we should like to point out some differences between the approach developed in the present study and the theoretical consideration of Hofman and Stein.[19] In fact, the general aim of both studies is similar: to investigate the effect of droplet deformability on the stability of emulsions. In both cases the Smoluchowski equation is considered as a starting point for examining the coagulation kinetics. However, Hofman and Stein[19] applied the Smoluchowski equation only to the case of *nondeformable droplets*. The deformability of the droplets is accounted for only when considering the energy of formation of a doublet of attached particles, like those shown in Figure 2. The thickness of the film during the deformation is assumed to remain constant. In this respect their model[19] is quite similar to

(41) Haber, S.; Hetsroni, G.; Solan, A. *Int. J. Multiphase Flow* **1973**, *1*, 57.
(42) van den Tempel, M. *Recueil* **1953**, *72*, 433.
(43) Danov, K.; Ivanov, I.; Gurkov, T.; Borwankar, R. Submitted for publication in *J. Colloid Interface Sci.*
(44) Schowalter, W. R. *Annu. Rev. Fluid Mech.* **1984**, *16*, 245.
(45) Kumar, S.; Kumar, R.; Gandhi, K. S. *Chem. Eng. Sci.* **1991**, *46*, 2483: *Chem. Eng. Sci.* **1992**, *47*, 971.

the one used in our previous study[15] where the effect of droplet deformability on the energy of particle interaction and second osmotic viral coefficient in microemulsions was investigated. Such an approach is appropriate for estimation of the equilibrium properties but it should be extended to the investigation of the droplet coalescence kinetics in emulsions, because it entirely ignores the dynamics of the processes—the rate of film drainage and rupture, the hydrodynamic interactions before and after deformation, etc. In this respect we believe that the approach developed in the present article is a self-consistent modification of the Smoluchowski scheme for the case of deformable coalescing droplets. On the other hand, we are aware that for complete estimation of the rate of coalescence in a particular system one should provide an additional analysis of the possibility for rupture of the layer between the droplets prior to the formation of planar film, $h_{cr} > h_i$. Since a theory for h_{cr} in the case of spherical droplets is still not available, we cannot say whether this possibility can be realized in miniemulsions. Such an analysis is under way and will be published soon.

5. Concluding Remarks

In the present study we extend the Smoluchowski scheme for particle coagulation to the case of coalescing deformable emulsion droplets. The overall picture of the process includes several consecutive stages: (i) close approach of nondeformed droplets; (ii) formation and expansion of plane-parallel film; (iii) thinning of the film at almost constant radius; (iv) rupture of the film and fusion of the droplets into a larger one—see Figure 1. In every one of these stages the intermolecular and hydrodynamics interactions are considered separately. By using appropriate expression for the droplet interactions and boundary conditions of the Smoluchowski type, we calculated the distance at which the droplet deformation takes place (see eqs 3.20–3.22), the two-particle nonequilibrium (but steady) radial distribution function (eq 2.9) and the total force (including the average Brownian force) which acts between the droplets (eq 2.14). As a result, the particle flux toward a given "central" droplet, i.e. the coalescence rate, can be determined; see eqs 2.4–2.6 and 2.22–2.23.

Most of the numerical results are devoted to calculation of the particle separation, h_i, at which the deformation occurs. The latter depends on the droplet interactions: van der Waals, electrostatic, hydrodynamic, as well as on the energy for deformation of the droplets. The influence of different factors (Hamaker constant, surface potential, interfacial tension, droplet size, and others) is investigated—see Figures 3–6. It is shown that the attraction between the droplets increases h_i, while the repulsion leads to the opposite effect. Besides, at large enough electrostatic repulsion, the deformation can become improbable and the droplets behave as nondeformable charged spheres (see Figure 5). The numerical calculations show that for micrometer size droplets and absence of electrostatic repulsion, the rate-determining stage is the approach of the particles before their deformation. For microemulsion droplets the deformability slows down the coalescence (see Figure 8). In the calculations we accounted for the interaction through the planar film as well as for the interaction between the parts of the deformed spheres outside the film because they give comparable contribution.

Acknowledgment. This work was financially supported by Kraft General Foods, Inc.